Asian Journal of Chemistry; Vol. 36, No. 10 (2024), 2475-2484

ASIAN JOURNAL OF CHEMISTRY

https://doi.org/10.14233/ajchem.2024.32318

Molecular Docking and ADME Profiles of Hyrtiosulawesine Derivatives Targeting pfLDH: Exploring Potential as Antimalarial Agents

SITI ZAFIRAH ZULKIFLI[1,2], AHMAD AMZAR ABDUL AZIZ[3], AIMI SUHAILY SAAIDIN[1], NURASYIKIN HAMZAH[3] and NOOR HIDAYAH PUNGOT[1,2,*]

[1]Organic Synthesis Laboratory, Institute of Science (IOS), Universiti Teknologi MARA, Puncak Alam Campus, 42300 Bandar Puncak Alam, Selangor, Malaysia
[2]Faculty of Applied Sciences, Universiti Teknologi MARA, 40450, Shah Alam, Selangor, Malaysia
[3]Department of Chemistry, Kulliyyah of Science, International Islamic University Malaysia (IIUM) 25200 Kuantan, Pahang, Malaysia

*Corresponding author: E-mail: noorhidayah977@uitm.edu.my

Received: 15 July 2024; *Accepted*: 25 September 2024; *Published online*: 30 September 2024; AJC-21780

The relentless rise in *Plasmodium falciparum*'s resistance to existing antimalarial drugs has sparked an urgent quest for novel therapeutic agents. For centuries, natural resources have been the bedrock of medicinal remedies, with β-carboline emerging as a beacon of hope in antimalarial research. In this study, we delve into the potential of hyrtiosulawesine derivatives as revolutionary antimalarial compounds, utilizing hyrtiosulawesine as the crucial scaffold. Employing a sophisticated amalgamation of molecular docking and ADME (absorption, distribution, metabolism and excretion) profiling, we meticulously screened an extensive library of hyrtiosulawesine's derivatives against *P. falciparum*. Based on advanced computational techniques, the binding affinities and interaction profiles were assessed and culminating in the selection of the most promising candidates based on their exceptional binding interactions. Moreover, the comprehensive ADME analyses were performed to assess the pharmacokinetic properties of these derivatives, ensuring their suitability as drug candidates. The results showed that most of the analogues exhibited strong binding affinities (-7.2 to -9.8 kcal/mol) to the *Plasmodium falciparum* lactate dehydrogenase (pfLDH) protein, surpassing that of hyrtiosulawesine itself. Among these, compounds **2t** and **1w** demonstrated the strongest binding, likely due to hydrogen bonding with Arg171 and Asn197. ADME profiling revealed that all hyrtiosulawesine derivatives displayed favourable drug-likeness properties and adhered to the Lipinski Rule of 5 (Ro5) indicating their potential efficacy as antimalarial agents. This investigation provides a foundation for further *in vitro* and *in vivo* investigations paving the way for the development of effective treatments against malaria.

Keywords: ADME, Antimalarial, Hyrtiosulawesine analogues, Molecular docking.

INTRODUCTION

Malaria remains a colossal global health menace, especially ravaging developing nations with its most devastating toll in sub-Saharan Africa, where countless children under the age of five succumb to this relentless scourge [1]. The crisis has deteriorated over time as the parasites evolve and develop resistance to current antimalarial treatments [2]. Chloroquine, the pioneering antimalarial drug of the late 1950s, initially spearheaded the fight against malaria [3]. However, cunning parasite mutations have conferred resistance by curtailing chloroquine accumulation in the vacuole, severely undermining its efficacy [4]. This resistance phenomenon has ominously extended to other frontline treatments such as sulfadoxine-pyrimethamine, mefloquine and even artemisinin. In response, the scientific community is persistently striving to develop new antimalarial drugs, aiming to diminish both the morbidity and mortality inflicted by this enduring plague.

Natural products have long been a treasure trove of therapeutic agents, with marine organisms presenting a vast and largely uncharted reservoir of bioactive compounds [5]. Among these natural resources, artemisinin, derived from the plant *Artemisia annua* also known as sweet wormwood or Qinghao in traditional Chinese medicine has emerged as a potent antimalarial remedy [6]. This discovery was catalyzed by the mounting resistance to previous antimalarial drugs such as chloro-

quine, sulfadoxine-pyrimethamine, mefloquine and quinine. While full resistance to artemisinin has not yet been reported, reports of delayed parasite clearance times have sparked concerns about the diminishing efficacy of artemisinin based combination therapies (ACTs) [7]. Consequently, researchers have turned its gaze to the vast potential of natural compounds and their derivatives, seeking to bolster the potency and longevity of ACTs.

Various naturally occurring alkaloids with β-carboline, dihydro-β-carboline or tetrahydro-β-carboline frameworks, exhibit formidable efficacy against malaria [8]. A standout example is manzamine, an alkaloid intricately combining a β-carboline with a complex pentacyclic diamine ring system, commanding considerable acclaim for its potent antimalarial properties [9]. The isolation of manzamine A, a new anticancer alkaloid, in the Okinawa marine sponge (Haliclona) by Sakai *et al*. [10] in 1986 was a major development in the field. Subsequent investigations have extended to encompass other β-carboline derivatives such as hyrtiosulawesine, sourced from marine sponges *Hyrtio erectus* and *Hyrtio reticulatus*, alongside the botanical treasure *Alocasia macrorrhiza* [11]. These compounds have shown great potential in the treatment of malaria due to their inhibitory effects on plasmodium parasites.

To expedite the investigation, analogues of hyrtiosulawesine are currently undergoing screening through a blend of molecular docking and ADME analysis. Molecular docking stands as a robust method enabling the prediction of how small molecules bind and orient themselves within specific protein active sites, thereby illuminating their potential as therapeutic agents [12]. Beyond binding affinity, the ADME profiles of these derivatives are evaluated to confirm favourable pharmacokinetic attributes essential for efficacy and safety as medicinal compounds. This integrated computational strategy represents an essential initial phase in the drug discovery process, guiding the identification of candidates poised for further experimental validation.

EXPERIMENTAL

Ligand preparation: Hyrtiosulawesine and its analogues (Fig. 1) were selectively designed and illustrated using ChemDraw Pro 16.0. Their 3D structures were generated with Chem-3D 16.0 and energy minimization was performed using the same software. The optimized ligands were individually saved in PDB format and then used in AutoDockTools (ADT) 1.5.6 [13]. The Gasteiger charges were calculated and the files were saved in PDBQT format for molecular docking analysis.

Protein preparation: The target enzyme chosen pfLDH (PDB ID: 1U4S) was obtained from the Protein Data Bank at a resolution of 2.0 Å. Initially, the water molecules and co-crystallized ligands were removed from its crystal structure. Polar hydrogen atoms and Kollman charges were subsequently added using ADT 1.5.6. The optimized protein structure was then saved in PDBQT format for subsequent molecular docking investigations.

Defining grid box for docking: A grid box was created using AutoGrid in ADT 1.5.6 to encompass all amino acid residues within the active site of interest, including the area

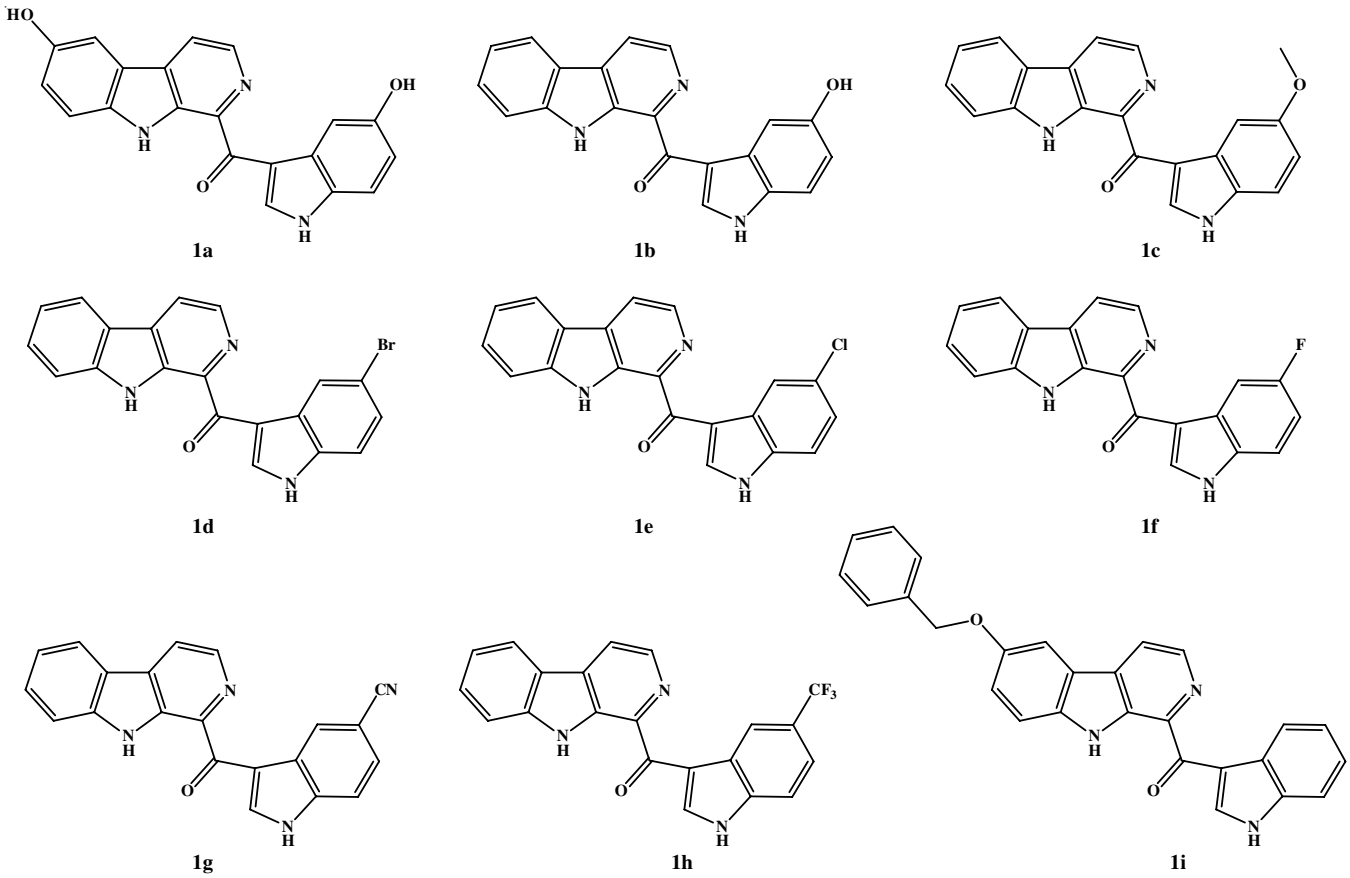

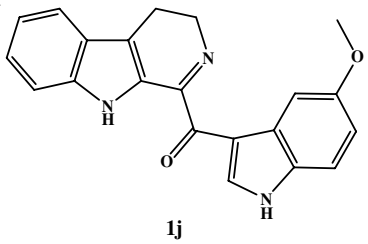

1j

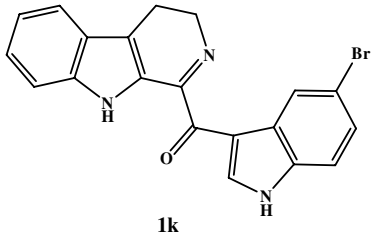

1k

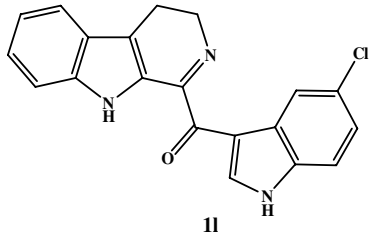

1l

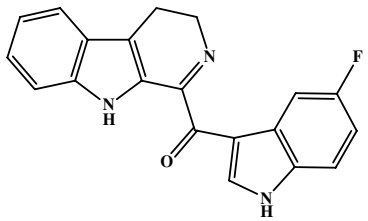

1m

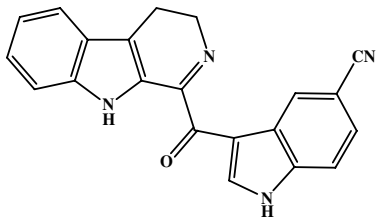

1n

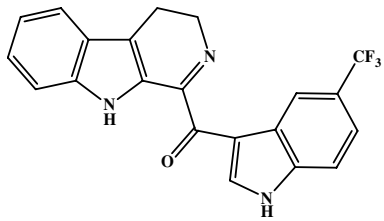

1o

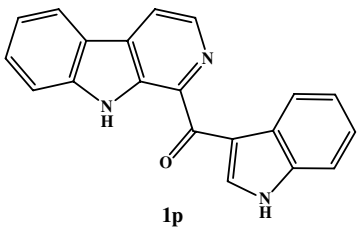

1p

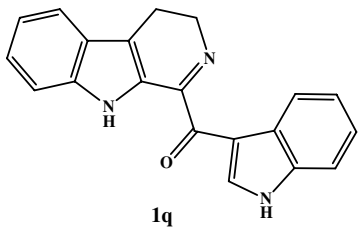

1q

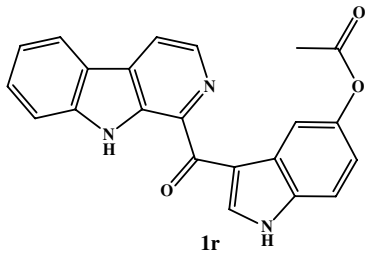

1r

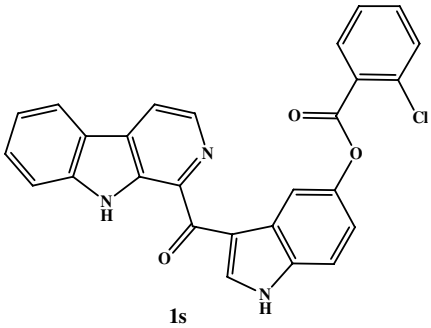

1s

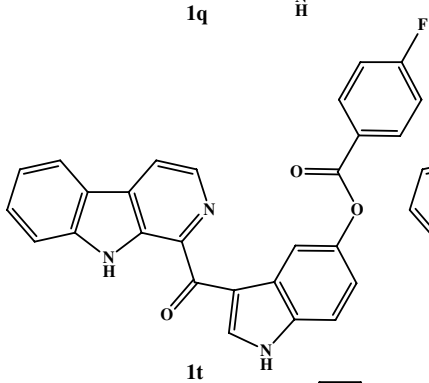

1t

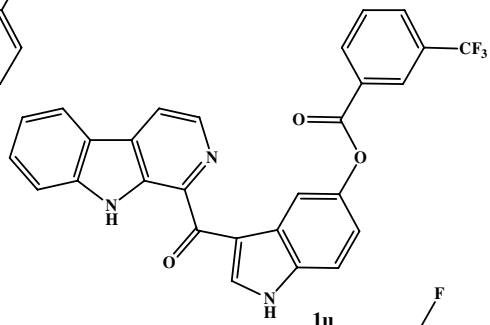

1u

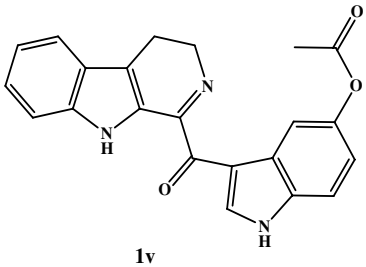

1v

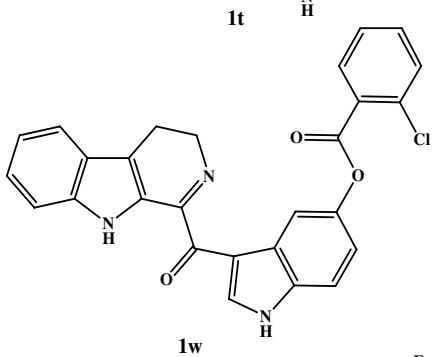

1w

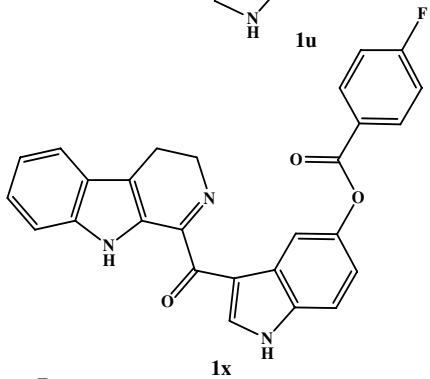

1x

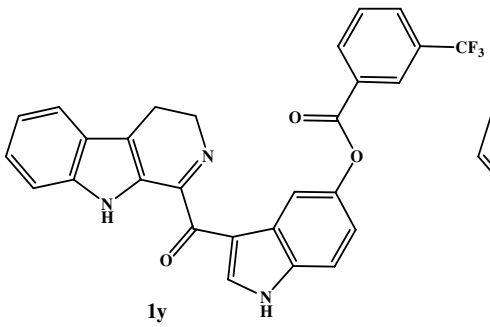

1y

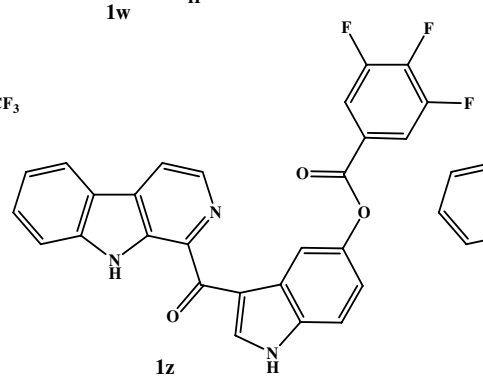

1z

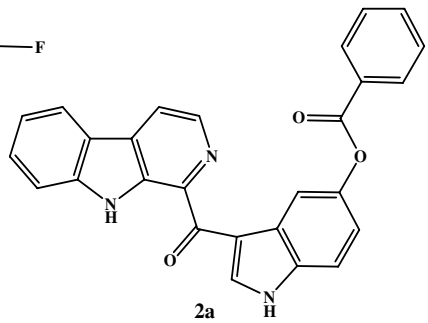

2a

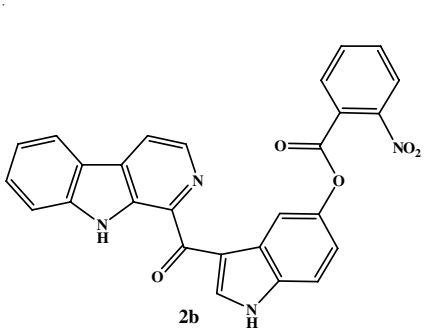

2b

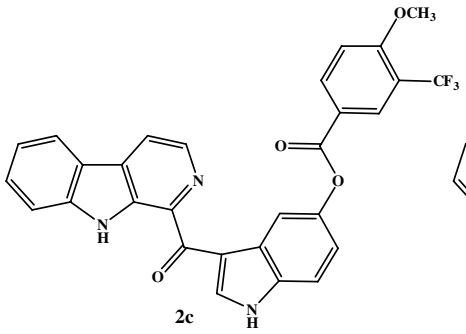

2c

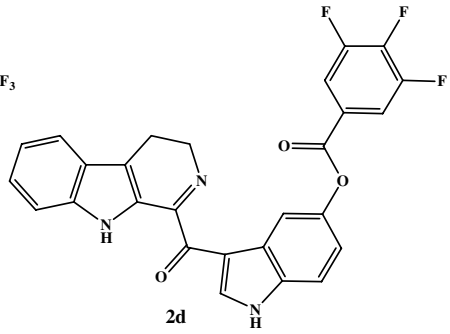

2d

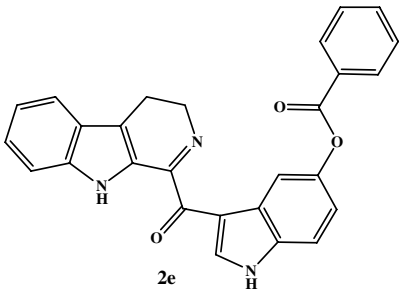

2e

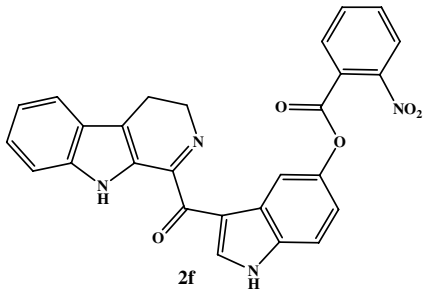

2f

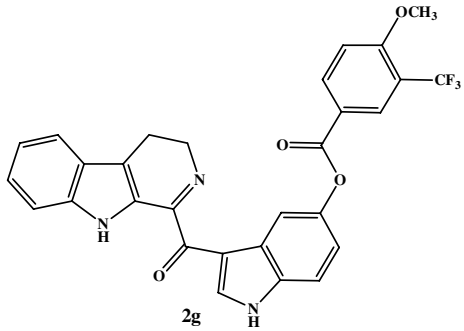

2g

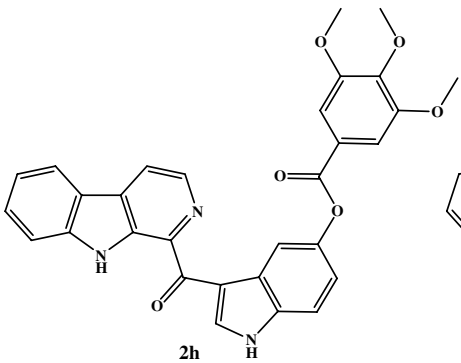

2h

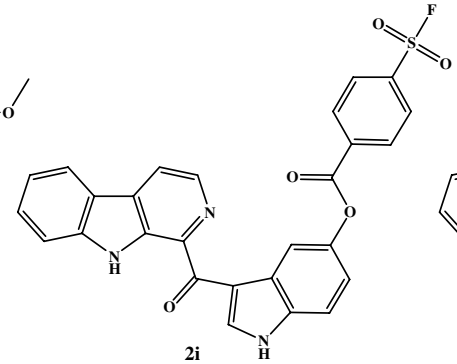

2i

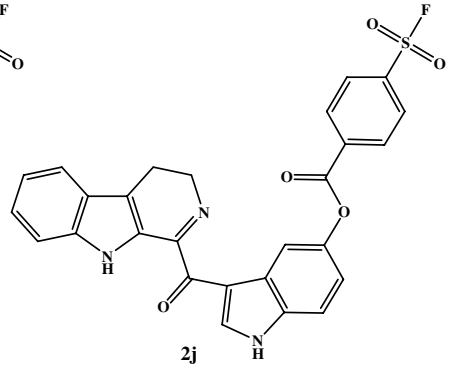

2j

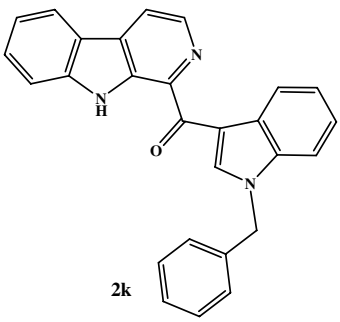

2k

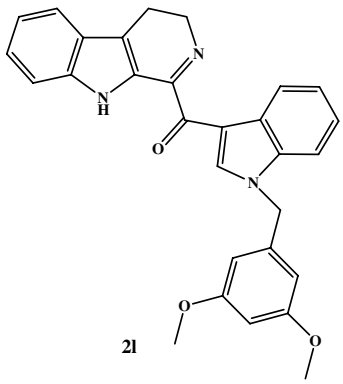

2l

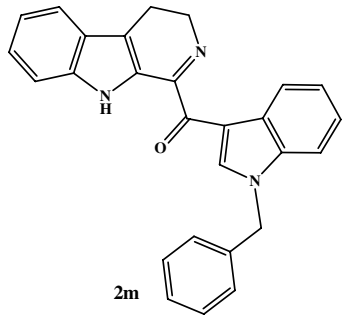

2m

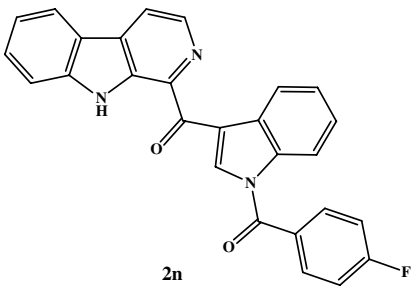

2n

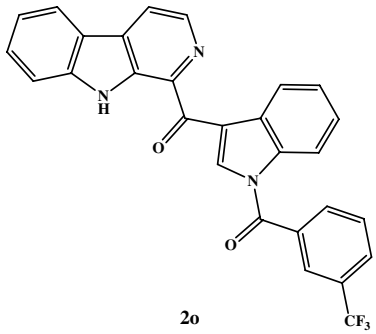

2o

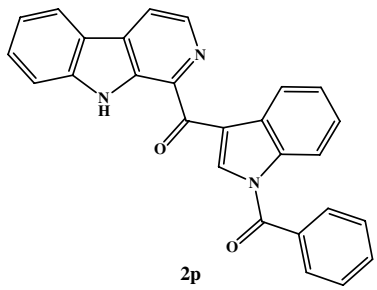

2p

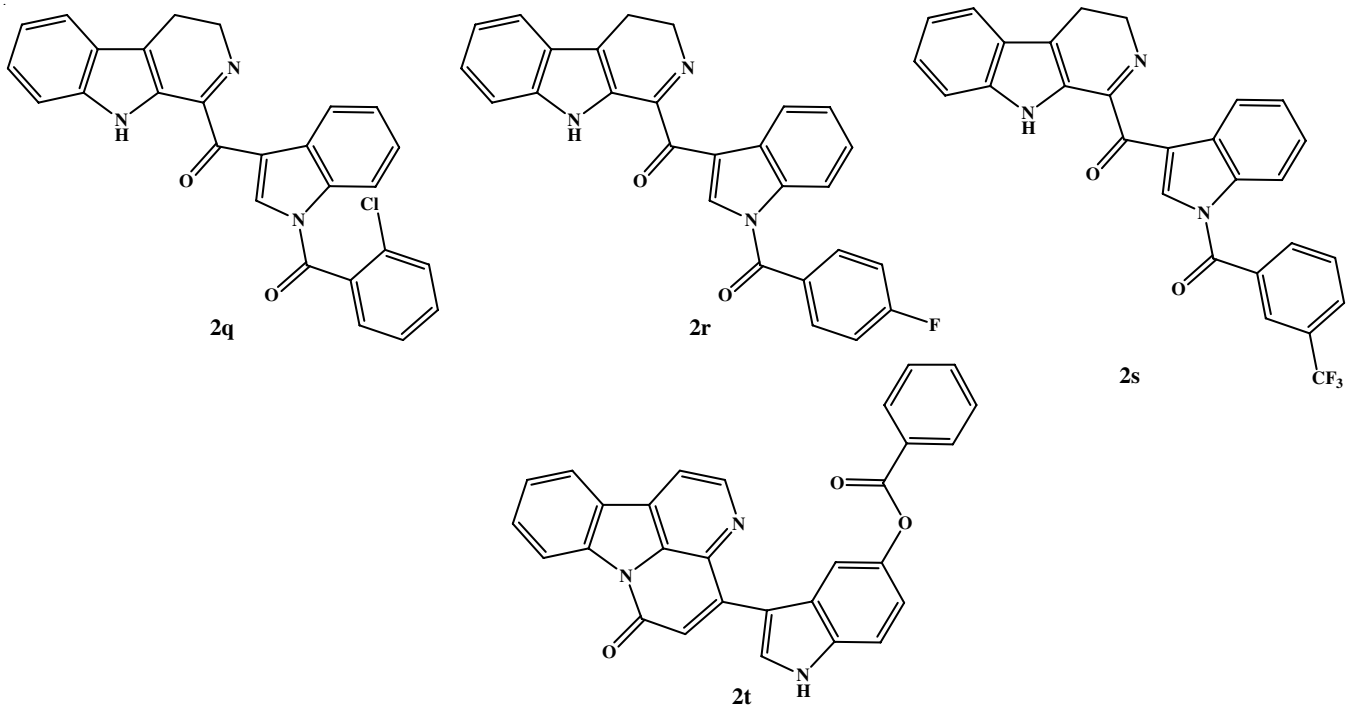

Fig. 1. Chemical structures for *in silico* molecular docking analysis

occupied by the co-crystallized ligand (naphthalene-2,6-disulfonic acid). The dimensions of the grid cavity were 8 Å × 14 Å × 8 Å, centered at coordinates 23.587 × 17.939 × 5.185 along the *x*, *y* and *z*-axes, respectively. A grid spacing of 1.0 Å was set to ensure sufficient coverage and resolution for accurate docking calculations.

Molecular docking: Molecular docking analysis was conducted using AutoDock Vina 1.5.6, employing a genetic algorithm for its search method and semi-empirical approaches to compute free energy as its scoring function. Prior to docking, input configuration files were prepared, including protein and ligand structures in PDBQT format, along with defined grid coordinates. The docking parameters were set with 10 modes, an energy range of 4 and exhaustiveness set to 100. The process was executed *via* command mode and results were assessed based on the binding affinity values (kcal/mol). Additionally, Discovery Studio and PyMOL were utilized for 2D and 3D visualization to analyze chemical interactions, including the hydrogen bonds, hydrophobic interactions and bond distances [14].

***In silico* ADME profiling:** Physiochemical evaluation plays a pivotal role in assessing the potential drug-likeness of compounds, predicting crucial parameters such as absorption, distribution, metabolism and excretion (ADME) [15]. Drug-likeness scores for all analogues were determined using the SwissADME server, inputting SMILES notations generated during ligand preparation. According to Lipinski's Rule of Five (Ro5), drug-like compounds must adhere to specific parameters: molecular weight (g/mol), number of hydrogen bond donors (HBD), number of hydrogen bond acceptors (HBA), topological polar surface area (TPSA), x log P calculation (Log P), with allowance for no more than one violation.

RESULTS AND DISCUSSION

The molecular docking process commenced with a meticulous validation between the protein and its native ligand. As Fig. 2 illustrates, the triumphant redocking of naphthalene-2,6-disulfonic acid achieved an RMSD value of 0.694, well below the 2 Å threshold, thereby showcasing the impeccable precision of the docking methodology. The docked molecule's position was strikingly identical to that of the native ligand in the protein's X-ray crystal structure, underscoring the accuracy of this approach [16]. All the subsequent docking studies rigorously adhered to this protocol, with their binding affinities, ranging from the most potent to the least, extensively recorded in Table-1.

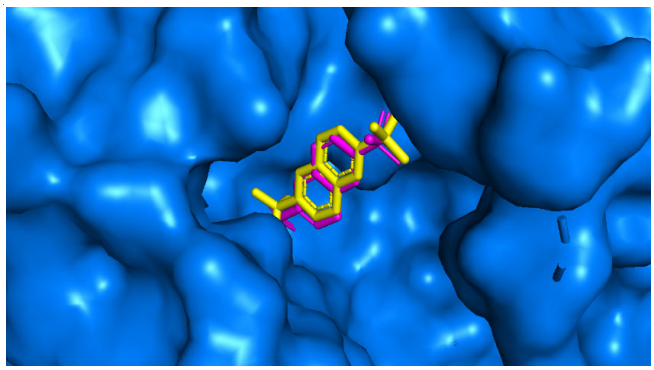

Fig. 2. Superposition of naphthalene-2,6-disulfonic acid (pink) as bound and redocked native ligand (yellow)

Table-1 presents an illustrious ranking of binding affinities for all ligands, meticulously ordered from the highest to the lowest binding energy, along with the amino acid residues

TABLE-1
MOLECULAR DOCKING RESULTS OF HYRTIOSULAWESINE AND ITS DERIVATIVES

Compounds	Binding affinities (kcal/mol)	Amino acid residue having interaction within 4 Å distance
3-(6-Oxo-6*H*-indolo[3,2,1-*de*][1,5]naphthyridin-4-yl)-1*H*-indol-5-yl benzoate (**2t**)	-9.7	Arg171, Ala236, Asn197, Gly196, Asn140
3-(4,9-Dihydro-3*H*-pyrido[3,4-*b*]indole-1-carbonyl)-1*H*-indol-5-yl 2-chlorobenzoate (**1w**)	-9.0	Asn140, Arg171, Ala236, Asn197, Val233, Gly196
3-(9*H*-Pyrido[3,4-*b*]indole-1-carbonyl)-1*H*-indol-5-yl 2-nitrobenzoate (**2b**)	-8.9	Asn140, Arg171, Ala236, Val233, Asn197, Gly196
(3-(9*H*-Pyrido[3,4-*b*]indole-1-carbonyl)-1*H*-indol-1-yl)(4-fluorophenyl)methanone (**2n**)	-8.8	Ala236, Asp168, Arg171, Asn140, Phe100
(3-(9*H*-Pyrido[3,4-*b*]indole-1-carbonyl)-1*H*-indol-1-yl)(phenyl)methanone (**2p**)	-8.8	Asn140, Gly196, Ala236
(4,9-Dihydro-3*H*-pyrido[3,4-*b*]indol-1-yl)(1-(3-(trifluoromethyl)benzoyl)-1*H*-indol-3-yl)methanone (**2s**)	-8.8	Ala236, Gly196, Asn140, Met325
(4,9-Dihydro-3*H*-pyrido[3,4-*b*]indol-1-yl)(1-(4-fluorobenzoyl)-1*H*-indol-3-yl)methanone (**2r**)	-8.7	Asn140, Arg171
3-(4,9-Dihydro-3*H*-pyrido[3,4-*b*]indole-1-carbonyl)-1*H*-indol-5-yl 3-(trifluoromethyl)benzoate (**1y**)	-8.6	Ala236, Val233, Asn197, Gly196
(1-(2-Chlorobenzoyl)-1*H*-indol-3-yl)(4,9-dihydro-3*H*-pyrido[3,4-*b*]indol-1-yl)methanone (**2q**)	-8.5	Ala236, Met325, Gly196
3-(9*H*-Pyrido[3,4-*b*]indole-1-carbonyl)-1*H*-indol-5-yl 3-(trifluoromethyl)benzoate (**1u**)	-8.4	Asn140, Arg171, Ala236, Asn197, Val233, Gly196
3-(9*H*-Pyrido[3,4-*b*]indole-1-carbonyl)-1*H*-indol-5-yl 4-fluorobenzoate (**1t**)	-8.1	Asn140, Arg171, Ala236
3-(4,9-Dihydro-3*H*-pyrido[3,4-*b*]indole-1-carbonyl)-1*H*-indol-5-yl 4-fluorobenzoate (**1x**)	-8.1	Asn140, Arg171, Ala236, Asn197
3-(9*H*-Pyrido[3,4-*b*]indole-1-carbonyl)-1*H*-indol-5-yl 4-methoxy-3-(trifluoromethyl)benzoate (**2c**)	-8.1	Asn140, Arg171, His195
3-(4,9-Dihydro-3*H*-pyrido[3,4-*b*]indole-1-carbonyl)-1*H*-indol-5-yl 2-nitrobenzoate (**2f**)	-8.1	Asn140, Arg171, Ala236, Asn197
(3-(9*H*-Pyrido[3,4-*b*]indole-1-carbonyl)-1*H*-indol-1-yl)(3-(trifluoromethyl)phenyl)methanone (**2o**)	-8.1	Ala236, Asp168, Arg171, Asn140
3-(9*H*-Pyrido[3,4-*b*]indole-1-carbonyl)-1*H*-indol-5-yl 3,4,5-trifluorobenzoate (**1z**)	-8.0	Asn140, Arg171, Ala236
3-(4,9-Dihydro-3*H*-pyrido[3,4-*b*]indole-1-carbonyl)-1*H*-indol-5-yl 3,4,5-trifluorobenzoate (**2d**)	-8.0	Asn140, Arg171, Ala236, Asn197
3-(4,9-Dihydro-3*H*-pyrido[3,4-*b*]indole-1-carbonyl)-1*H*-indol-5-yl 4-(fluorosulfonyl)benzoate (**2j**)	-8.0	Gly196, Arg171
(1-Benzyl-1*H*-indol-3-yl)(9*H*-pyrido[3,4-*b*]indol-1-yl)methanone (**2k**)	-8.0	Asn140, His195
(4,9-Dihydro-3*H*-pyrido[3,4-*b*]indol-1-yl)(1-(3,5-dimethoxybenzyl)-1*H*-indol-3-yl)methanone (**2l**)	-8.0	Asn140, His195, Asn197, Gly196
(1-Benzyl-1*H*-indol-3-yl)(4,9-dihydro-3*H*-pyrido[3,4-*b*]indol-1-yl)methanone (**2m**)	-8.0	Asn140, Gly196, His195,
3-(9*H*-Pyrido[3,4-*b*]indole-1-carbonyl)-1*H*-indol-5-yl benzoate (**2a**)	-7.9	Asn140, Arg171, Ala236
3-(4,9-Dihydro-3*H*-pyrido[3,4-*b*]indole-1-carbonyl)-1*H*-indol-5-yl benzoate (**2e**)	-7.9	Asn140, Arg171, Ala236, Asn197
3-(9*H*-Pyrido[3,4-*b*]indole-1-carbonyl)-1*H*-indol-5-yl 4-(fluorosulfonyl)-benzoate (**2i**)	-7.8	Gly196, Ala236, Arg171
3-(9*H*-Pyrido[3,4-*b*]indole-1-carbonyl)-1*H*-indol-5-yl 2-chlorobenzoate (**1s**)	-7.7	Asn140, Arg171, Ala236
3-(4,9-Dihydro-3*H*-pyrido[3,4-*b*]indole-1-carbonyl)-1*H*-indol-5-yl 4-methoxy-3-(trifluoromethyl)benzoate (**2g**)	-7.7	Thr101, Asn140, Arg171, Ala236
(4,9-Dihydro-3*H*-pyrido[3,4-*b*]indol-1-yl)(5-(trifluoromethyl)-1*H*-indol-3-yl)methanone (**1o**)	-7.6	Asn140, Asn197, Ala236
3-(9*H*-Pyrido[3,4-*b*]indole-1-carbonyl)-1*H*-indol-5-yl acetate (**1r**)	-7.6	Asn140, Arg171, Ala236
(6-(Benzyloxy)-9*H*-pyrido[3,4-*b*]indol-1-yl)(1H-indol-3-yl)methanone (**1i**)	-7.5	Arg171, Ala236, Asn197
(5-Bromo-1*H*-indol-3-yl)(9*H*-pyrido[3,4-*b*]indol-1-yl)methanone (**1d**)	-7.4	Ala236, Arg171
(4,9-Dihydro-3*H*-pyrido[3,4-*b*]indol-1-yl)(5-methoxy-1*H*-indol-3-yl)methanone (**1j**)	-7.4	Ala236, Arg171
(9*H*-Pyrido[3,4-*b*]indol-1-yl)(5-(trifluoromethyl)-1*H*-indol-3-yl)methanone (**1h**)	-7.4	Ala236, Asn140
3-(4,9-Dihydro-3*H*-pyrido[3,4-*b*]indole-1-carbonyl)-1*H*-indole-5-carbonitrile (**1n**)	-7.4	Asn197, Ala236
3-(9*H*-Pyrido[3,4-*b*]indole-1-carbonyl)-1*H*-indole-5-carbonitrile (**1g**)	-7.4	Ala236, Arg171
(5-Bromo-1*H*-indol-3-yl)(4,9-dihydro-3*H*-pyrido[3,4-*b*]indol-1-yl)methanone (**1k**)	-7.3	Asn197, Ala236, Asn140
(5-Chloro-1*H*-indol-3-yl)(4,9-dihydro-3*H*-pyrido[3,4-*b*]indol-1-yl)methanone (**1l**)	-7.3	Asn197, Ala236, Asn140
(4,9-Dihydro-3*H*-pyrido[3,4-*b*]indol-1-yl)(5-fluoro-1*H*-indol-3-yl)methanone (**1m**)	-7.3	Asn140, Ala 236, Val 233
(4,9-Dihydro-3*H*-pyrido[3,4-*b*]indol-1-yl)(1H-indol-3-yl)methanone (**1q**)	-7.3	Asn140, Val233, Ala236
3-(4,9-Dihydro-3*H*-pyrido[3,4-*b*]indole-1-carbonyl)-1*H*-indol-5-yl acetate (**1v**)	-7.3	Asn140, Arg171, Ala236
(5-Hydroxy-1*H*-indol-3-yl)(6-hydroxy-9*H*-pyrido[3,4-*b*]indol-1-yl)methanone (**1a**)	-7.2	Arg109, Gly196, Arg171, Ala236
(5-Hydroxy-1*H*-indol-3-yl)(9*H*-pyrido[3,4-*b*]indol-1-yl)methanone (**1b**)	-7.2	Asn140, Ala236, Arg171
(5-Methoxy-1*H*-indol-3-yl)(9*H*-pyrido[3,4-*b*]indol-1-yl)methanone (**1c**)	-7.2	Asn140, Ala236, Arg171
(5-Chloro-1*H*-indol-3-yl)(9*H*-pyrido[3,4-*b*]indol-1-yl)methanone (**1e**)	-7.2	Ala236, Arg171,
(5-Fluoro-1*H*-indol-3-yl)(9*H*-pyrido[3,4-*b*]indol-1-yl)methanone (**1f**)	-7.2	Asn140, Ala236, Arg171
(4,9-Dihydro-3*H*-pyrido[3,4-*b*]indol-1-yl)(5-methoxy-1*H*-indol-3-yl)methanone (**1j**)	-7.2	Ala236, Asn140
3-(9*H*-Pyrido[3,4-*b*]indole-1-carbonyl)-1*H*-indol-5-yl 3,4,5-trimethoxybenzoate (**2h**)	-7.2	Asn140, His195, Ala236, Arg171
(1H-Indol-3-yl)(9*H*-pyrido[3,4-*b*]indol-1-yl)methanone (**1p**)	-7.0	Ala 236, Arg 171
Naphthalene-2,6-disulfonic acid	-5.2	Arg 171, Asn 140

involved in the binding interactions within a 4 Å distance. The molecular docking studies have shown that nearly all analogues exhibit strong binding to the DNA protein, with binding energies ranging from -7.2 kcal/mol to -9.7 kcal/mol. In contrast, the native ligand, naphthalene-2,6-disulfonic acid, displayed more modest binding values (~ -5.2 kcal/mol). The hyrtiosulawesine derivatives (**2t**) demonstrated the most significant binding interactions with the protein, requiring the additional examination. Compounds **1w** and **2b** also demonstrated better interactions, solidifying their importance in this study.

The 3D representation of the DNA gyrase-ligand complex revealed a breathtaking panorama where all the target compounds magnificently docked at the protein's active site (Fig. 3a). Derivative **2t** exhibited the highest binding affinities and showed few interactions including pi-sigma, pi-donor hydrogen bonds, van der Waals forces and hydrogen bonds. The hydrogen bonding interactions were observed between the oxygen and nitrogen atoms of the ligand and the amino acids of Arg171 and Asn197 residues (Fig. 3b). In a similar manner, compound **1w** engaged with Arg171 and Asn197, as well as Val233 residues, through the formation of hydrogen bonds between the amine groups in the scaffold (Fig. 3c). Mirroring the grandeur of compound **1w**, hydrogen bonding was observed through Arg171, Asn197 and Val233 of compound **2b**, with an additional interaction at Asn140 adding to the complexity. In a striking contrast, naphthalene-2,6-disulfonic acid (Fig. 3e) displayed the same hydrogen bonding interactions between Arg171 residues and two oxygen atoms of sulfonic acid attached to the naphthalene backbone (Fig. 3e).

Interestingly, the pocket fit the hyrtiosulawesine analogues well, particularly analogues **2t**, **1w** and **2b**, which demonstrated the comparable binding affinities observed (-8.9 to -9.7 kcal/mol) (Fig. 3a). From the 2D representations (Fig. 3), it is illustrated that all three derivatives showed the same interaction involving the amine moieties in the scaffold with Arg171 and Asn197 *via* hydrogen bonding. However, the presence of chlorine and nitrogen attached to benzoyl chloride substituents, that fit into the deep pocket of the DNA gyrase, making -NH of β-carboline ring interacting with Val233 and Asn140 residue through the formation of additional hydrogen bonds (Fig. 3b) while compared to compound **2t** (- 9.7 kcal/mol). In addition to all the derivatives docked, the O- and N- acylation of benzoyl group were found to have good interaction compared to the unsubstituted of acylation group indole, suggesting potential for synthesizing similar compounds in the future. Even so, the 5-substituted indole ring is also providing a good interaction of binding affinities.

***In silico* ADME assessment:** *In silico* ADME (absorption, distribution, metabolism and excretion) assessment employs advanced computational techniques and models to forecast the pharmacokinetic behaviour of drug candidates. This methodology is crucial for modern drug discovery and development,

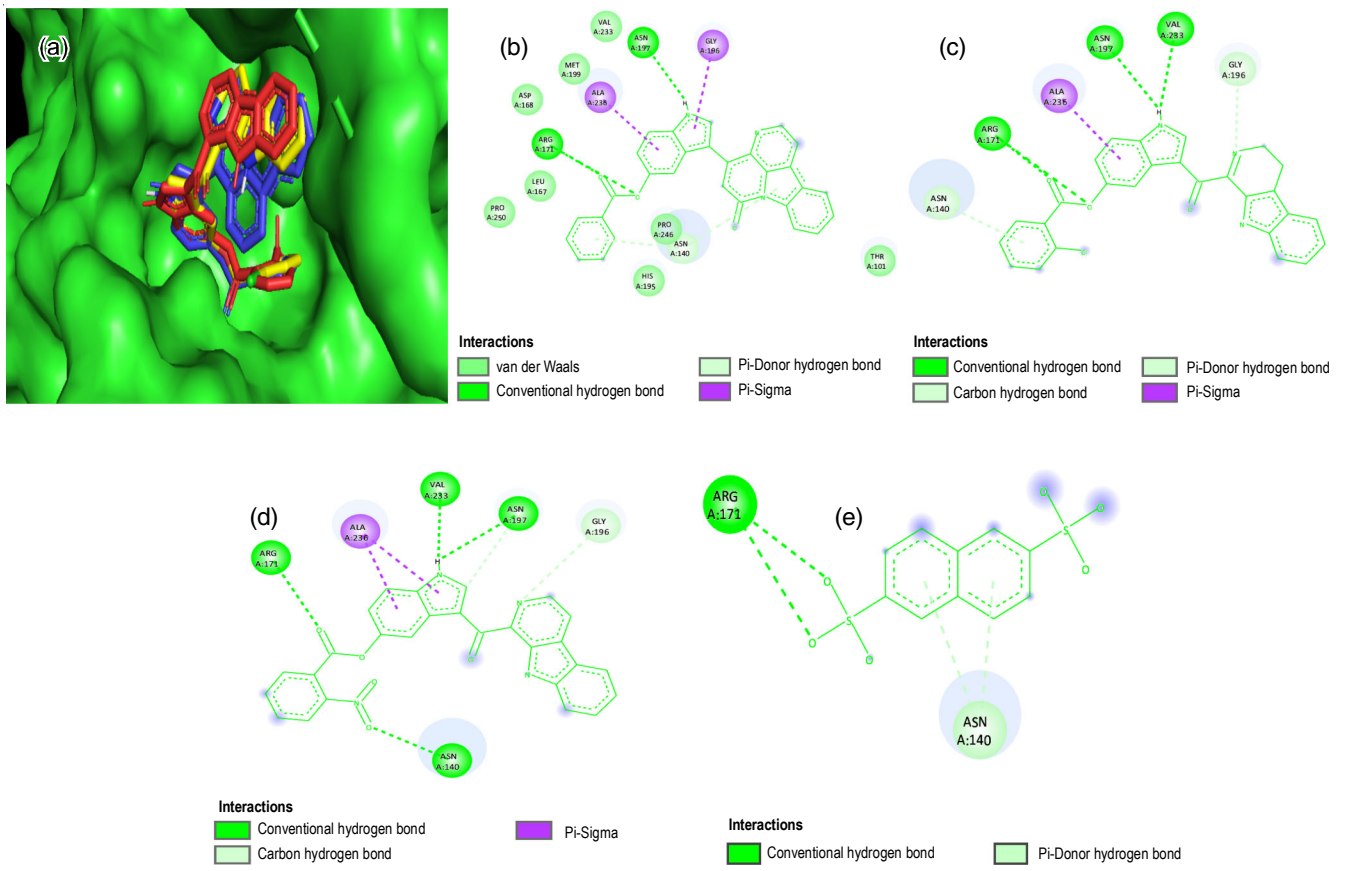

Fig. 3. (a) 3D representation showing the docking poses of highest interaction ligands of **2t** (blue), **1w** (yellow) and **2b** (red) docked at DNA gyrase active site and 2D bonding interactions of compound (b) **2t**, (c) **1w**, (d) **2b** and (e) naphthalene-2,6-disulfonic acid. The distance between amino acid residues and the ligand was set to less than 4 Å

enabling rapid evaluation of potential drug interactions within the body, hence avoiding costly and time-consuming *in vitro* and *in vivo* experiments [17,18]. One of the prevalent tools in this domain, SwissADME, meticulously analyses each descriptor to determine whether a chemical compound satisfies the drug-likeness criteria established by experts like Lipinski, Ghose, Veber, Egan and Muegge [19].

The 'Rule of 5' (Ro5) parameters encompass several critical factors, including molecular weight (g/mol), the number of hydrogen bond donors (HBD), the number of hydrogen bond

TABLE-2
ADME ASSESSMENT OF HYRTIOSULAWESINE'S DERIVATIVES

Compound	MW (< 500 g/mol)	Log P < 5	TPSA < 140 Å^2	HBA < 10	HBD < 5	Lipinski rule
1a	343.34	1.68	102.00	4	4	Yes; 0 violation
1b	327.34	2.06	81.77	3	3	Yes; 0 violation
1c	341.36	2.60	70.77	3	2	Yes; 0 violation
1d	390.23	2.75	61.54	2	2	Yes; 0 violation
1e	345.79	2.64	61.54	2	2	Yes; 0 violation
1f	329.33	2.43	61.54	3	2	Yes; 0 violation
1g	336.35	2.24	85.33	3	2	Yes; 0 violation
1h	379.33	2.57	61.54	5	2	Yes; 0 violation
1i	417.46	3.00	70.77	3	2	Yes; 0 violation
1j	343.38	2.40	70.24	3	2	Yes; 0 violation
1k	392.25	2.42	61.01	2	2	Yes; 0 violation
1l	347.80	2.31	61.01	2	2	Yes; 0 violation
1m	331.34	2.14	61.01	3	2	Yes; 0 violation
1n	338.36	1.95	84.80	3	2	Yes; 0 violation
1o	381.35	2.20	61.01	5	2	Yes; 0 violation
1p	311.34	1.89	61.54	2	2	Yes; 0 violation
1q	313.35	1.97	61.01	2	2	Yes; 0 violation
1r	369.37	2.51	87.84	4	2	Yes; 0 violation
1s	465.89	3.06	87.84	4	2	Yes; 0 violation
1t	449.43	2.78	87.84	5	2	Yes; 0 violation
1u	499.44	3.34	87.84	7	2	Yes; 0 violation
1v	371.39	2.34	87.31	4	2	Yes; 0 violation
1a	343.34	1.68	102.22	4	4	Yes; 0 violation
1w	467.90	3.21	87.31	4	2	Yes; 0 violation
1x	451.45	2.96	87.31	5	2	Yes; 0 violation
1y	501.46[a]	3.25	87.31	7	2	Yes; 1 violation
1z	485.41	2.70	87.84	7	2	Yes; 0 violation
2a	431.44	3.08	87.84	4	2	Yes; 0 violation
2b	476.44	2.58	133.66	6	2	Yes; 0 violation
2c	529.47	3.07	97.07	8	2	Yes; 1 violation
2d	487.43	3.08	130.78	7	2	Yes; 0 violation
2e	433.46	3.05	87.31	4	2	Yes; 0 violation
2f	478.46	2.71	133.13	6	2	Yes; 0 violation
2g	531.48	3.42	96.54	8	2	Yes; 1 violation
2h	521.52	3.36	115.53	7	2	Yes; 1 violation
2i	513.50	2.39	130.36	7	2	Yes; 1 violation
2j	515.51	2.89	129.83	7	2	Yes; 1 violation
2k	401.46	3.31	50.68	2	1	Yes; 0 violation
2l	463.53	3.53	68.61	4	1	Yes; 0 violation
2m	403.48	3.22	50.15	2	1	Yes; 0 violation
2n	433.43	3.27	67.75	4	1	Yes; 0 violation
2o	483.44	2.92	67.75	6	1	Yes; 0 violation
2p	415.44	3.04	67.75	3	1	Yes; 0 violation
2q	451.90	3.53	67.22	3	1	Yes; 0 violation
2r	435.45	3.18	67.22	4	1	Yes; 0 violation
2s	485.46	3.43	67.22	6	1	Yes; 0 violation
2t	455.46	3.27	76.46	4	1	Yes; 0 violation

Red: poor; Yellow: intermediate; Green: good

acceptors (HBA), topological polar surface area (TPSA) and the x log P calculation (LogP), with a stipulation that no more than one violation is permissible. Under the Ro5, the molecular weight (MW) should be less than 500 Daltons, compounds exceeding this threshold may struggle to traverse cell membranes, potentially impairing their absorption and distribution within the body [20]. Additionally, the LogP, the logarithm of the partition coefficient between n-octanol and water, quantifies a compound's hydrophobicity. A LogP value over 5 indicates excessive hydrophobicity, which can result in poor absorption and solubility challenges. Furthermore, the number of hydrogen bond donors (HBD), defined as the sum of OH and NH groups in a molecule, should be under 5, as excessive hydrogen bonding can obstruct a compound's ability to cross cell membranes. Conversely, the number of hydrogen bond acceptors (HBA) must be fewer than 10, as a high HBA count can also impede membrane permeability.

According to Table-2, hyrtiosulawesine and its derivatives have successfully navigated the rigorous criteria of the Lipinski Rule of 5 (Ro5), thus affirming their potential for oral administration. Notably, while most derivatives comply with the Ro5, certain exceptions such as **1y**, **2c**, **2g**, **2h**, **2i** and **2j** slightly exceed the molecular weight threshold of 500 Daltons while still adhering to Lipinski's guidelines. Additionally, all derivatives demonstrate satisfactory flexibility, although compounds **2b**, **2d** and **2i** exhibit lower polar surface areas. The Ro5 stipulates that effective orally administered drugs typically adhere to no more than one of the following: fewer than five hydrogen bond donors (HBD), fewer than 10 hydrogen bond acceptors (HBA), a molecular weight under 500 Daltons and a *c*LogP (lipophilicity) not exceeding five.

Conclusion

The molecular docking analysis of hyrtiosulawesine and its analogues targeting DNA gyrase unveiled significantly enhanced binding affinities, ranging from -7.3 kcal/mol to -9.8 kcal/mol, surpassing that of naphthalene-2,6-disulfonic acid at -5.2 kcal/mol. Remarkably, compound **2t** emerged as the standout with the highest binding affinity at -9.8 kcal/mol, attributed to robust hydrogen bonding interactions with Arg 171 and Asn197 residues. Following closely, compounds **1w** and **2b** also demonstrated superior interactions compared to hyrtiosulawesine itself, forming additional hydrogen bonds with Asn140 and Val233 residues. Moreover, extensive in silico ADME analyses confirmed that hyrtiosulawesine analogues strictly comply with the rigorous Lipinski Rule of 5 (Ro5) criteria, supporting their suitability for oral administration. These findings highlight compound **2t** as a potential option for antimalarial therapy targeting DNA gyrase, due to its favourable ADME profile and remarkable binding affinity.

ACKNOWLEDGEMENTS

This work was financially supported under the Fundamental Research Grant Scheme (FRGS/1/2022/STG04/UITM/02/7) funded by the Ministry of Education, Malaysia.

CONFLICT OF INTEREST

The authors declare that there is no conflict of interests regarding the publication of this article.

REFERENCES

1. H.J. Oladipo, Y.A. Tajudeen, I.O. Oladunjoye, S.I. Yusuff, R.O. Yusuf, E.M. Oluwaseyi, M.O. Abdul Basit, Y.A. Adebisi and M.S. El-Sherbini, *Ann. Med. Surg.*, **81**, 104366 (2022); https://doi.org/10.1016/j.amsu.2022.104366
2. C.H. Sibley, *Mol. Biochem. Parasitol.*, **195**, 107 (2014); https://doi.org/10.1016/j.molbiopara.2014.06.001
3. E.G. Tse, M. Korsik and M.H. Todd, *Malar. J.*, **18**, 93 (2019); https://doi.org/10.1186/s12936-019-2724-z
4. D.A. Fidock, T. Nomura, A.K. Talley, R.A. Cooper, S.M. Dzekunov, M.T. Ferdig, L.M.B. Ursos, A.B.S. Sidhu, B. Naudé, K.W. Deitsch, X. Su, J.C. Wootton, P.D. Roepe and T.E. Wellems, *Mol. Cell*, **6**, 861 (2000); https://doi.org/10.1016/S1097-2765(05)00077-8
5. A. Choudhary, L.M. Naughton, I. Montánchez, A.D.W. Dobson and D.K. Rai, *Mar. Drugs*, **15**, 272 (2017); https://doi.org/10.3390/md15090272
6. H.N. ElSohly, E.M. Croom Jr., F.S. El-Feraly and M.M. El-Sherei, *J. Nat. Prod.*, **53**, 1560 (1990); https://doi.org/10.1021/np50072a026
7. World Health Organization (WHO), Artemisinin and Artemisinin-based Combination Therapy Resistance: Status Report No. WHO/HTM/GMP/2016.11 (2016).
8. A. Kamboj, B. Sihag, D.S. Brar, A. Kaur and D.B. Salunke, *Eur. J. Med. Chem.*, **221**, 113536 (2021); https://doi.org/10.1016/j.ejmech.2021.113536
9. P. Ashok, S. Ganguly and S. Murugesan, *Drug Discov. Today*, **19**, 1781 (2014); https://doi.org/10.1016/j.drudis.2014.06.010
10. R. Sakai, T. Higa, C.W. Jefford and G. Bernardinelli, *J. Am. Chem. Soc.*, **108**, 6404 (1986); https://doi.org/10.1021/ja00280a055
11. S.Z. Zulkifli, N.H. Pungot, A.S. Saaidin, N.A. Jani and M.F. Mohammat, *Nat. Prod. Res.*, 1 (2023); https://doi.org/10.1080/14786419.2023.2261141
12. P.C. Agu, C.A. Afiukwa, O.U. Orji, E.M. Ezeh, I.H. Ofoke, C.O. Ogbu, E.I. Ugwuja and P.M. Aja, *Sci. Rep.*, **13**, 13398 (2023); https://doi.org/10.1038/s41598-023-40160-2
13. G.M. Morris, R. Huey, W. Lindstrom, M.F. Sanner, R.K. Belew, D.S. Goodsell and A.J. Olson, *J. Comput. Chem.*, **30**, 2785 (2009); https://doi.org/10.1002/jcc.21256
14. L. Schrödinger and W. DeLano, PyMOL (2020); http://www.pymol.org/pymol
15. P. Sucharitha, K.R. Reddy, S.V. Satyanarayana, and T. Garg, Eds.: A. Parihar, R. Khan, A. Kumar, A.K. Kaushik and H. Gohel, Absorption, Distribution, Metabolism, Excretion and Toxicity Assessment of Drugs using Computational Tools, In: Computational approaches for Novel Therapeutic and Diagnostic Designing to Mitigate SARS-CoV-2 Infection, Academic Press, Chap. 5, pp. 335-355 (2022).
16. E. López-Camacho, M.J. García-Godoy, J. García-Nieto, A.J. Nebro, and J.F. Aldana-Montes, Eds.: Botón-Fernández, M., Martín-Vide, C., Santander-Jiménez, S., Vega-Rodríguez, M.A., A New Multi-objective Approach for Molecular Docking Based on RMSD and Binding Energy. In: Algorithms for Computational Biology. AlCoB 2016. Lecture Notes in Computer Science, Vol. 9702, pp. 65-77 (2016).

17. E. Anklam, M.I. Bahl, R. Ball, R.D. Beger, J. Cohen, S. Fitzpatrick, P. Girard, B. Halamoda-Kenzaoui, D. Hinton, A. Hirose, A. Hoeveler, M. Honma, M. Hugas, S. Ishida, G.E.N. Kass, H. Kojima, I. Krefting, S. Liachenko, Y. Liu, S. Masters, U. Marx, T. McCarthy, T. Mercer, A. Patri, C. Pelaez, M. Pirmohamed, S. Platz, A.J.S. Ribeiro, J.V Rodricks, I. Rusyn, R.M. Salek, R. Schoonjans, P. Silva, C.N. Svendsen, S. Sumner, K. Sung, D. Tagle, L. Tong, W. Tong, J. van den Eijnden-van-Raaij, N. Vary, T. Wang, J. Waterton, M. Wang, H. Wen, D. Wishart, Y. Yuan and W. Slikker Jr., *Exp. Biol. Med.*, **247**, 1 (2002); https://doi.org/10.1177/15353702211052280
18. J. Gan, B. Bolon, T.V. Vleet and C. Wood, eds.: W.M. Haschek, C.G. Rousseaux and M.A. Wallig; In Haschek and Rousseaux's Handbook of Toxicologic Pathology, pp. 925-966 (2022).
19. A. Daina, O. Michielin and V. Zoete, *Sci. Rep.*, **7**, 42717 (2017); https://doi.org/10.1038/srep42717
20. C.M. Nisha, A. Kumar, P. Nair, N. Gupta, C. Silakari, T. Tripathi and A. Kumar, *Bioinform. Adv.*, **2016**, 9258578 (2016); https://doi.org/10.1155/2016/9258578